Journal of the European Ceramic Society 23 (2003) 809–815

www.elsevier.com/locate/jeurceramsoc

High-temperature mechanical properties of sinter-forged silicon nitride with ytterbia additive

Naoki Kondo*, Yoshikazu Suzuki, Tatsuya Miyajima, Tatsuki Ohji

Synergy Materials Research Center, National Institute of Advanced Industrial Science and Technology (AIST), Shimo-shidami 2268-1, Moriyama-ku, Nagoya 463-8687, Japan

Received 8 February 2002; received in revised form 15 May 2002; accepted 25 May 2002

Abstract

Anisotropic silicon nitride with ytterbia additive was successfully fabricated by using a sinter-forging technique. The sinter-forged specimen had a strongly anisotropic microstructure where rod-like silicon nitride grains preferentially aligned perpendicular to the forging direction. The specimen exhibited higher strength and higher fracture energy compared to the conventionally hot-pressed specimen. These superior mechanical properties of the sinter-forged silicon nitride were attributed to grain bridging and pullout enhanced by grain alignment. At elevated temperatures, softening of the grain boundary glassy phase and melting of the secondary crystalline phase should lead to degradation of strength and increment of fracture energy.

Keywords: Mechanical properties; Microstructure-final; Si_3N_4; Sinter forging

1. Introduction

In order to improve strength and fracture toughness of silicon nitride ceramics, many studies have been conducted to control their microstructures: grain size and morphology, grain alignment, and boundary chemistry.[1–7] Recently, grain alignment control to make anisotropic microstructure have been reported as a most promising technique to achieve, concurrently, both high strength and high toughness in specific directions. There are two major routes to fabricate such anisotropic silicon nitrides: one is tape-casting and another is forging. By aligning rod-like silicon nitride grains using a tape-casting technique with seed particles, Hirao et al.[8] obtained high strength of about 1.1 GPa and high fracture toughness of about 11 MPa $m^{1/2}$ when stress was applied parallel to, or a crack extended normal to, the grain alignment. Present authors succeeded in alignment of rod-like silicon nitride grains by using a superplastic forging[9] or superplastic sinter-forging[10] techniques. In these studies, rod-like silicon nitride grains were aligned by forging, resulted in strongly anisotropic microstructure formation. Strength and fracture toughness of the forged one were approximately 1.65 GPa and 13 MPa $m^{1/2}$, respectively, when a stress was applied parallel to the alignment (strong direction). Those of the sinter-forged one, which consisted of smaller grains than the forged one, were approximately 2.1 GPa and 8 MPa $m^{1/2}$, respectively. Even at elevated temperatures, the anisotropic silicon nitride, fabricated by superplastic forging,[9] showed high strength and fracture energy.[11] Overall the temperature range from R.T. to 1300 °C, strength and fracture energy of the anisotropic one were 1.5–2 and 3.5–8 times higher than those of isotropic one, respectively. However, containing 5 wt.% Y_2O_3 and 3 wt.% Al_2O_3 as sintering additives, the grain boundary glassy phase was consequently softened and strength was degraded at high temperatures above 1100 °C. The high temperature mechanical properties can be improved by choosing sintering additives and making a refractory grain boundary phase.[12–14] It has been known that ytterbia (Yb_2O_3) is a most promising additive for this purpose since it leads to good oxidation resistance[13] and high temperature strength.[14]

In this study, the authors intend to produce silicon nitride with aligned rod-like grains by using Yb_2O_3

* Corresponding author. Tel.: +81-52-739-0156; fax: +81-52-739-0136.

E-mail address: naoki-kondo@aist.go.jp (N. Kondo).

0955-2219/02/$ - see front matter © 2002 Elsevier Science Ltd. All rights reserved.
PII: S0955-2219(02)00189-9

additives and sinter-forging technique. Then, strength and fracture energy of the fabricated specimen at elevated temperatures up to 1500 °C, as well as at room temperature, are investigated. Because of its anisotropic microstructure and controlled grain boundary glassy phase, the specimen can be expected to show better mechanical properties than those of the previous study[11] at elevated temperatures.

2. Experimental procedures

2.1. Sample fabrication

Referring to previous studies,[12–18] α-silicon nitride powder (E10, Ube Industries. Ltd., Tokyo, Japan), 13 wt.% Yb_2O_3 (99.99%, 2 μm, Kojundo Chemical Laboratory, Tokyo, Japan) and 2 wt.% SiO_2 (99.9%, 0.8 μm, Kojundo Chemical Laboratory, Tokyo, Japan) were mixed. This composition ideally forms Si_3N_4 and Yb_2SiO_5 as crystalline phases. The mixed powder was ball-milled for 50 h in methanol using silicon nitride balls, then dried and sieved.

Powder was compacted using a steel die, followed by a cold isostatic pressing (CIP) with a pressure of 98 MPa. Dimensions and relative density of the CIP body were 40×40×15 mm and about 52%, respectively. The CIP body was sinter-forged using a graphite die of 45×45 mm in the base and in a graphite resistance furnace. The atmosphere inside the furnace, nitrogen gas (99.99%) under 0.9 MPa pressure, was maintained throughout the process. Sinter-forging was conducted at 1900 °C for 3 h, and both heating and cooling rates were 10 °C min^{-1}. After heating to the desired temperature, mechanical pressure of approximately 30 MPa was applied for 3 h. For comparison, several specimens were fabricated by usual hot-pressing at 1900 °C for 3 h under 30 MPa. Obtained samples were heat-treated at 1400 °C for 24 h to crystallize the glassy phase at triple points.[12] Thereafter, the sinter-forged and hot-pressed specimens were designated as SF-SN and HP-SN, respectively. Planes normal and parallel to the pressing direction are designated as top and side planes, respectively.

2.2. Mechanical testing

Densities of fabricated specimens were calculated dividing weight by dimension. X-ray diffraction analysis was conducted to identify phases of specimen, as well as to examine orientation of silicon nitride grains. Specimens of 3×4×45 mm for measuring bending strength were cut from the sintered body so that the stress face was perpendicular to the pressing direction. All faces were finished lengthwise by a 400 grid diamond wheel; edges were chamfered using an 800 grid diamond whetstone. Elastic modulus was measured using four point bending technique with a strain gauge. Three-point bending strength was measured with a span of 30 mm and a displacement rate of 0.5 mm min^{-1} at room temperature (R.T.), 1200, 1300, 1400, and 1500 °C, in air.

Fracture energy was measured by using chevron-notched beam (CNB) method. This technique was employed for two reasons. One is that the crack extends in a stable manner until final failure. Another is that the crack extends macroscopically by Mode I due to ligament configuration; otherwise a crack tends to deflect along aligned grains. Details of the employed CNB specimen geometry and testing procedures were the same as those of the previous study.[19] The CNB specimen had dimensions of 4×3×45 mm with regular triangle shaped ligament (edge length was 3 mm). Initial crack length was 1.4 mm and width of the chevron-notch was 0.1 mm. Measurement was performed in three-point bending with a span of 30 mm and a displacement rate of 0.01 mm min^{-1} at room temperature (R.T.), 1400 and 1500 °C, in air. To examine the effect of oxidation, some additional measurements were conducted in nitrogen atmosphere. Fractured surfaces of CNB specimens were observed by scanning electron microscopy (SEM).

3. Results and discussion

3.1. Sample fabrication

The SF-SN body is exhibited together with the CIP body in Fig. 1. The SF-SN body had approximate dimensions of 45×45×6 mm. No cracking was observed on the SF-SN surface. Densities of HP-SN and SF-SN were 3.352 and 3.345 kg m^{-3}, respectively, and they were about 97% of theoretical density.[18] In X-ray diffraction analysis, β-Si_3N_4 (JCPDS card 33–1160), Yb_2SiO_5 (JCPDS 40–0386), and $Yb_2Si_2O_7$ (JCPDS 25–1345) were detected in fabricated specimens, as shown in Fig. 2. The powder mixture was designed to form Si_3N_4 and Yb_2SiO_5 as crystalline phases. However, as a surface oxidized film (silica film) usually exists on the silicon nitride powder, some more oxygen should be

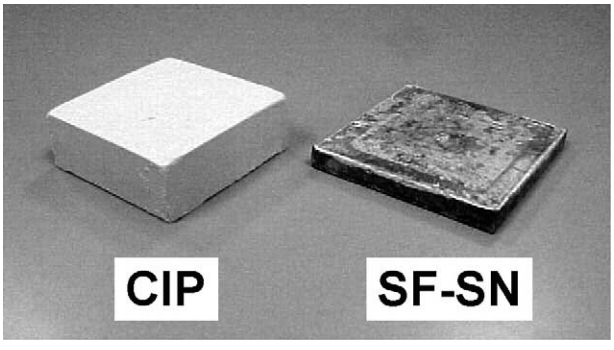

Fig. 1. CIP and SF-SN bodies.

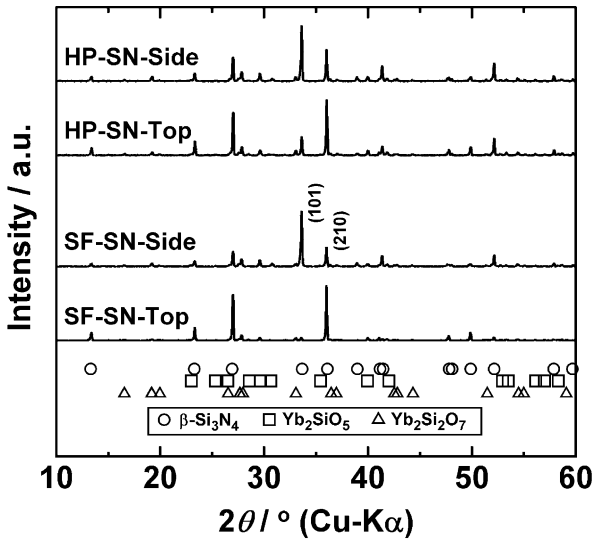

Fig. 2. X-ray diffraction analysis of HP-SN and SF-SN specimens.

contained in the powder mixture. Thus the crystalline phases, β-Si_3N_4, Yb_2SiO_5, and $Yb_2Si_2O_7$ were detected in the actual sintered body.[12,17,18] These phases seemed to form after devitrification of the glassy phase. As can be understood from a phase diagram[20] and microstructure observation,[21] glassy phase existed at the sinter-forging temperature. The minor crystalline phases, Yb_2SiO_5 and $Yb_2Si_2O_7$, possibly formed, but the amount of them should be little. This glassy phase seemed to allow the sinter-forging process without cracking.

Microstructures of HP-SN and SF-SN, which were taken from the fractured surfaces of CNB specimens (to be described later), are shown in Fig. 3. Both of the specimens mainly consisted of rod-like silicon nitride grains. Grains of HP-SN align slightly while those of SF-SN do so strongly and perpendicularly to the pressing direction. Both microstructures also showed protruding rod-like grains as well as holes or hollows.

Alignment is revealed more clearly by X-ray diffraction analysis (Fig. 2). X-ray diffraction analysis has been widely used to examine silicon nitride anisotropy (grain alignment);[22–29] some analyses discussed its relation to microstructural change. One typical value indicating anisotropy is the peak intensity ratio of (101)/(210).[24,25] In isotropic silicon nitride, (101) and (210) peaks should have approximately equal heights; the ratio of (101)/(210) is 1.06 (JCPDS card 33-1160). On the contrary, as known in Fig. 2, diffraction patterns from top and side planes of fabricated specimens were quite different; i.e., the (210) peak was remarkably higher in the top plane and lower in the side plane than the (101) peak. The (101)/(210) ratios from top planes were 0.33 and 0.05 for HP-SN and SF-SN, respectively. This result indicates that the prismatic plane of the silicon nitride grains tended to align perpendicularly to the pressing direction in the fabricated specimens. Anisotropy of SF-SN was much higher than that of HP-SN. In the case of hot-pressing, densification and grain growth occur rather concurrently, resulting in lower anisotropy. On the contrary, in sinter-forging, rod-like grains are formed during heating, and grains are aligned during sinter-forging by mechanical pressure, resulting in higher anisotropy. In addition, material flow during sinter-forging processing contributes substantially to grain alignment. Basal area of SF-SN was approximately 25% larger than that of the original CIP body. Thus, material flows perpendicularly to the pressing direction and rod-like grains naturally tend to align along the flow.[24]

Silicon nitrides used in previous studies[9,10,22–32] for obtaining anisotropic microstructures by forging or superplastic deformation mostly contained alumina as sintering additives. It has been known that alumina content leads to a grain boundary glassy phase with a

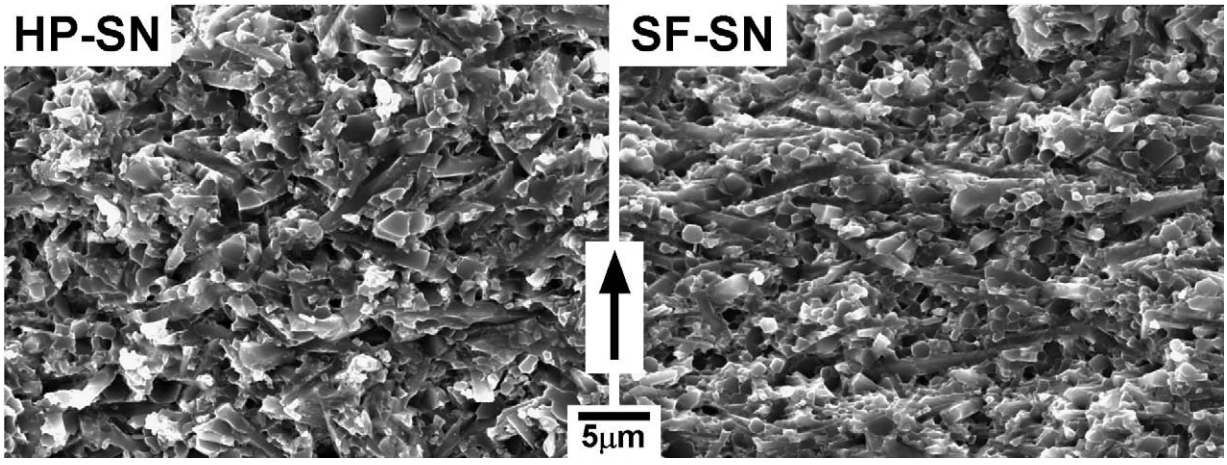

Fig. 3. Fractured surfaces of HP-SN and SF-SN CNB specimens. Pressing directions are vertical; arrow indicates crack propagation directions. Specimens were fractured at R.T.

low melting point, which enhances material flow in forging or superplastic deformation, but degrades high temperature mechanical properties. In this work, by choosing a suitable condition (i.e., amount and composition of additives, and sinter-forging temperature), anisotropic silicon nitride was successfully sinter-forged without alumina. Because of its anisotropic microstructure and grain boundary glassy phase without alumina, this specimen can be expected to show better mechanical properties than those of the previous study[11] at higher temperatures. High temperature mechanical properties of fabricated specimens are reported in the following section.

3.2. Mechanical testing

Elastic moduli of HP-SN and SF-SN, measured parallel to the top plane, were 301.9 and 326.1 GPa, respectively; the modulus of SF-SN was higher than that of HP-SN. The grain of β-silicon nitride itself has elastic anisotropy.[33] The elastic modulus is 450–540 and 280–310 GPa in directions parallel and perpendicular to the c-axis, respectively. Since silicon nitride grains were well-aligned parallel to the top plane in SF-SN, the high elastic modulus originated from elastic anisotropy of grains.

Fig. 4 shows temperature dependence of strength of HP-SN and SF-SN with standard deviations. Strength of SF-SN was 70–120 MPa higher than that of HP-SN throughout the temperature range of R.T. to 1500 °C. Due to softening of the grain boundary glassy phase, strength was degraded at elevated temperatures for both materials; i.e., SF-SN showed high strength of 1258 MPa at room temperature, gradually decreasing to 666 MPa at 1400 °C, then drastically decreasing to 441 MPa at 1500 °C. It has been reported that anisotropic silicon nitrides can show superior strength to isotropic ones at R.T. as well as at elevated temperatures since effective operation of grain bridging and pullout by grain alignment and disappearance of large defects all result in improved strength.[11,34] Similar mechanisms plausibly act in this case, resulting in higher strength in SF-SN.

In CNB tests, stable crack growth was obtained for every specimen until completion tests, except for HP-SN tested at 1400 °C. Load–displacement (L–D) curves for HP-SN and SF-SN at R.T. and 1500 °C are shown in Fig. 5. Since the elastic modulus of SF-SN is higher than that of HP-SN, the initial gradient of the curve for the former is slightly steeper than that for the latter at both temperatures. The gradient becomes shallow at 1500 °C due to softening of the grain boundary glassy phase. Peak load decreased, but the work of fracture (total energy under the L–D curve) increased at 1500 °C.

Fracture energy, γ_{eff}, is defined as

$$\gamma_{\text{eff}} = W_{\text{WOF}}/2A, \tag{1}$$

where W_{WOF} is the work of fracture and A is the area of the specimen web portion. Fig. 6 shows fracture energies of HP-SN and SF-SN calculated from L–D curves at R.T., 1400 and 1500 °C. Note that the error of this test was estimated to be 7% at most. Throughout the

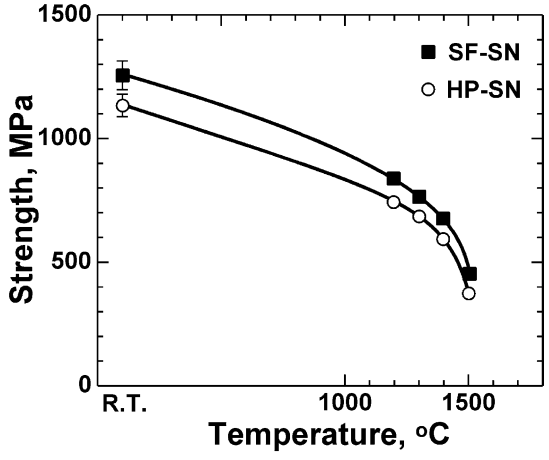

Fig. 4. High temperature strength of HP-SN and SF-SN specimens. Tests were conducted in air.

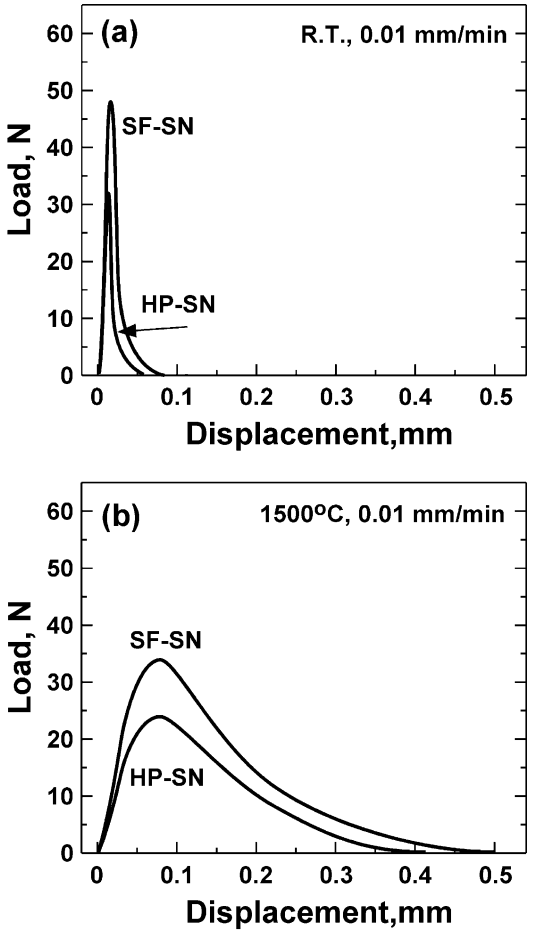

Fig. 5. L–D diagrams of CNB tests for HP-SN and SF-SN specimens: (a) R.T., (b) 1500 °C, in air.

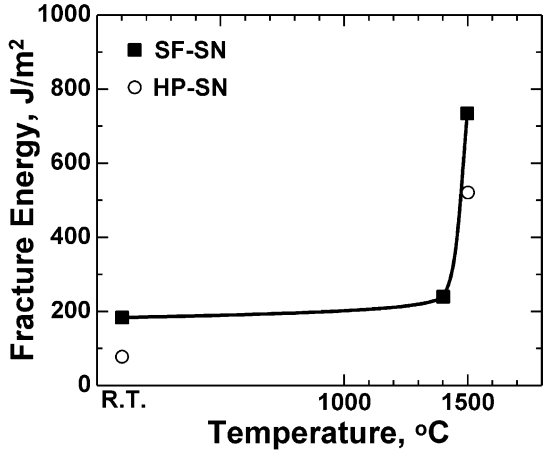

Fig. 6. High temperature fracture energies of HP-SN and SF-SN specimens. Tests were conducted in air.

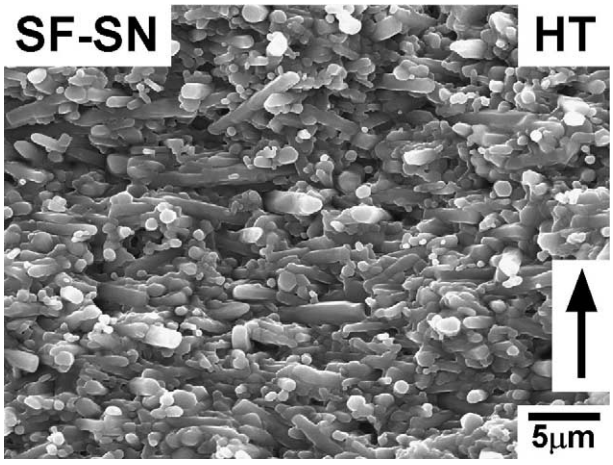

Fig. 7. Fractured surface of the SF-SN CNB specimen, tested at 1500 °C in a nitrogen atmosphere. Pressing direction is vertical; arrow indicates crack propagation direction.

temperature range of R. T. to 1500 °C, SF-SN showed higher fracture energy than HP-SN. Fracture energy of SF-SN was strongly affected by temperature; i.e. it slightly increased from 187 J/m^2 at R.T. to 235 J/m^2 at 1400 °C, and then steeply rose to 734 J/m^2 at 1500 °C. Though the stable fracture was not attained in HP-SN at 1400 °C, fracture energy at 1500 °C was substantially higher than that at R.T., similarly to SF-SN. There is some possibility that oxidation might affect fracture behavior, which leads to inflated *L–D* curves and larger fracture energies at 1500 °C. To assess this, additional CNB tests were conducted in a nitrogen atmosphere. Obtained fracture energies of HP-SN and SF-SN at 1500 °C were 570 and 753 J/m^2, respectively, which are slightly larger than those tested in air, suggesting little effect of oxidation. Fractured SF-SN surfaces are shown in Fig. 7. Comparing this surface to that tested at R.T. [Fig. 3(b)], grain pull-out is largely enhanced at 1500 °C. Thus, large fracture energies for both materials at high temperatures are primarily due to enhanced pull-out.

Silicon nitride is toughened primarily by crack wake toughening mechanisms including grain bridging and grain pullout.[35–37] As revealed in previous studies,[11,34,38] for anisotropic silicon nitrides, a greater number of rod-like grains are involved with the crack wake toughening mechanisms, resulting in high fracture energy. Grain bridging arises, particularly at R.T., from elastic deformation of rod-like grains that are partially debonded from the matrix. This toughening continues until grains are broken at some site within the debonded part and subsequently broken grain fragments are pulled-out from the matrix. For these to occur, interfacial debonding or partial fracture at the interface is essential; in grain pullout, at least at R.T., grains are not completely pulled out, but parts of them are. Protruding rod-like grains, mostly broken as shown in Fig. 3, support the above speculation.

In case of fracture at high temperatures, rod-like grains were almost completely pulled out as shown in Fig. 7; thus pullout can be considered to play a substantial role in toughening the material at high temperatures. At high temperatures where the grain boundary glassy phase is softened, viscoelastic properties become dominant and pullout presumably occurs due to failure through the viscous glassy phase rather than fracture at the interface. When a crack propagated and opened, rod-like grains of both sides of the crack were separated from each other without being broken through failure of viscous glassy phase. Large fracture energy, particularly at 1500 °C, is presumably attributable to sliding resistance during this pullout. On the other hand, grain bridging to the extent that the boundary is rigid enough to allow transmission of high elastic bridging stress is not likely to occur at high temperatures.

Fabricated silicon nitride with Yb_2O_3 additive showed superior high temperature mechanical properties compared to silicon nitride with Y_2O_3 and Al_2O_3 additives.[11] However, with increasing temperature from 1400 to 1500 °C, strength decreased and fracture energy increased drastically. Cinibulk et al.[21] reported that the melting temperature (eutectic point) of a minor crystalline phase, $Yb_2Si_2O_7$, of silicon nitride doped with 5 vol.% Yb_2O_3 and 0.5 vol.% Al_2O_3 was around 1470 °C. The above drastic changes of mechanical properties are very likely related to melting of minor crystalline phases.

4. Summary

Anisotropic silicon nitride with ytterbia additive was successfully fabricated using sinter-forging technique. The sinter-forged specimen had a strongly anisotropic microstructure where rod-like silicon nitride grains

preferentially aligned perpendicular to the forging direction. The specimen exhibited higher strength and higher fracture energy compared to the conventionally hot-pressed specimen. The sinter-forged specimen showed high strength of 1258 MPa at room temperature, which gradually decreased to 666 MPa at 1400 °C, then drastically decreased to 441 MPa at 1500 °C. Fracture energy exhibited 187 MPa $m^{1/2}$ at room temperature, which slightly increased to 235 MPa $m^{1/2}$ at 1400 °C, then radically jumped to 734 MPa $m^{1/2}$ at 1500 °C. High strength and high fracture energy of sinter-forged silicon nitride were attributed to grain bridging and pullout enhanced by grain alignment. At elevated temperatures, especially at 1500 °C, softening of grain boundary glassy phase and melting of secondary crystalline phases should lead to drastic changes in mechanical properties.

Acknowledgements

This work was supported by METI, Japan, as part of the Synergy Ceramics Project. The authors are members of the Joint Research Consortium of Synergy Ceramics.

References

1. Tani, E., Umebayashi, S., Kishi, K., Kobayashi, K. and Nishijima, M., Gas-pressure sintering of Si_3N_4 with concurrent addition of Al_2O_3 and 5 wt% rare earth oxide: high fracture toughness Si_3N_4 with fiber-like structure. *Am. Ceram. Soc. Bull.*, 1995, **65**(9), 1311–1315.
2. Kawashima, T., Okamoto, H., Yamamoto, H. and Kitamura, A., Grain size dependence of the fracture toughness of silicon nitride. *J. Ceram. Soc. Jpn.*, 1990, **98**(3), 235–242 (in Japanese).
3. Mitomo, M. and Uenosono, S., Microstructural development during gas-pressure sintering of α-silicon nitride. *J. Am. Ceram. Soc.*, 1992, **75**(1), 103–108.
4. Goto, Y. and Tsuge, A., Mechanical properties of unidirectionally oriented SiC-whisker reinforced Si_3N_4 fabricated by extrusion and hot-pressing. *J. Am. Ceram. Soc.*, 1993, **76**(1), 1420–1424.
5. Hirosaki, N., Akimune, Y. and Mitomo, M., Effect of grain grows of β-silicon nitride on strength, Weibull modulus and fracture toughness. *J. Am. Ceram. Soc.*, 1995, **78**(6), 1687–1690.
6. Becher, P. F., Lin, H. T., Hwang, S. L., Hoffmann, M. J. and Chen, I.-W., The influence of microstructure on the mechanical behavior of silicon nitride ceramics. In *Silicon Nitride Ceramics*, ed. I.-W. Chen, P. F. Becher, M. Mitomo, G. Petzow and T. S. Yen. Material Research Society, Pittsburgh, PA, 1993, pp. 147–158.
7. Hirao, K., Nagaoka, T., Brito, M. E. and Kanzaki, S., Microstructure control of silicon nitride by seeding with rodlike β-silicon nitride particles. *J. Am. Ceram. Soc.*, 1994, **77**(7), 1857–1862.
8. Hirao, K., Ohashi, M., Brito, M. E. and Kanzaki, S., Processing strategy for producing highly anisotropic silicon nitride. *J. Am. Ceram. Soc.*, 1995, **78**(6), 1687–1690.
9. Kondo, N., Ohji, T. and Wakai, F., Strengthening and toughening of silicon nitride by superplastic deformation. *J. Am. Ceram. Soc.*, 1998, **81**(3), 713–716.
10. Kondo, N., Suzuki, Y. and Ohji, T., Superplastic sinter-forging of silicon nitride with anisotropic microstructure formation. *J. Am. Ceram. Soc.*, 1999, **82**(4), 1067–1069.
11. Kondo, N., Inagaki, Y., Suzuki, Y. and Ohji, T., High-temperature fracture energy of superplastically forged silicon nitride. *J. Am. Ceram. Soc.*, 2001, **84**(8), 1791–1796.
12. Cinibulk, M. K. and Thomas, G., Fabrication and secondary-phase crystallization of rare-earth disilicate silicon-nitride ceramics. *J. Am. Ceram. Soc.*, 1992, **75**(8), 2037–2043.
13. Cinibulk, M. K., Thomas, G. and Johnson, S. M., Oxidation behavior of rare-earth disilicate silicon-nitride ceramics. *J. Am. Ceram. Soc.*, 1992, **75**(8), 2044–2049.
14. Cinibulk, M. K., Thomas, G. and Johnson, S. M., Strength and creep-behavior of rare-earth disilicate silicon-nitride ceramics. *J. Am. Ceram. Soc.*, 1992, **75**(8), 2050–2055.
15. Park, H., Kim, H. E. and Niihara, K., Microstructural evolution and mechanical properties of Si_3N_4 with Yb_2O_3 as a sintering additive. *J. Am. Ceram. Soc.*, 1997, **80**(3), 750–756.
16. Park, H., Kim, H. W. and Kim, H. E., Oxidation and strength retention of monolithic Si_3N_4 and nanocomposite Si_3N_4-SiC with Yb_2O_3 as a sintering aid. *J. Am. Ceram. Soc.*, 1998, **81**(8), 2130–2134.
17. Nishimura, T. and Mitomo, M., Phase-relationship in the system Si_3N_4-SiO_2-Yb_2O_3. *J. Mater. Res.*, 1995, **10**(2), 240–242.
18. Nishimura, T., Mitomo, M. and Suematsu, H., High temperature strength of silicon nitride ceramics with ytterbium silicon oxynitride. *J. Mater. Res.*, 1997, **12**(1), 203–209.
19. Ohji, T., Goto, Y. and Tsuge, A., High temperature toughness and tensile strength of whisker reinforced silicon nitride. *J. Am. Ceram. Soc.*, 1991, **74**(4), 739–745.
20. Levin, E. M., Robbins, C. R., McMurdie, H. F., ed., *Phase Equilibria Diagrams, Vol. II*. The American Ceramic Society, Columbus, OH, USA, 1969.
21. Cinibulk, M. K., Kleebe, H. J., Schneider, G. A. and Ruhle, M., Amorphous intergranular films in silicon-nitride ceramics quenched from high-temperatures. *J. Am. Ceram. Soc.*, 1993, **76**(11), 2801–2808.
22. Lee, F. and Bowman, K. J., Texture and anisotropy in silicon nitride. *J. Am. Ceram. Soc.*, 1992, **75**(7), 1748–1755.
23. Lee, F., Sandlin, M. S. and Bowman, K. J., Toughness anisotropy in textured ceramic composites. *J. Am. Ceram. Soc.*, 1993, **76**(7), 1793–1800.
24. Lee, F. and Bowman, K. J., Texture development via grain rotation in β-silicon nitride. *J. Am. Ceram. Soc.*, 1994, **77**(4), 947–953.
25. Yoon, S. Y., Akatsu, T. and Yasuda, E., Anisotropy of creep deformation rate in hot-pressed Si_3N_4 with preferred orientation of the elongated grains. *J. Mater. Sci.*, 1997, **32**(14), 3813–3819.
26. Wu, X. and Chen, I.-W., Exaggerated texture and grain growth in a superplastic SiAlON. *J. Am. Ceram. Soc.*, 1992, **75**(10), 2733–2741.
27. Hwang, S.-L. and Chen, I.-W., Superplastic forming of SiAlON ceramics. *J. Am. Ceram. Soc.*, 1994, **77**(10), 2575–2585.
28. Rouxel, T., Wakai, F. and Izaki, K., Tensile ductility of superplastic Al_2O_3-Y_2O_3-Si_3N_4/SiC composites. *J. Am. Ceram. Soc.*, 1992, **75**(9), 2363–2372.
29. Rouxel, T., Rossignol, F., Besson, J.-L. and Goursat, P., Superplastic forming of an alpha-phase rich silicon nitride. *J. Mater. Res.*, 1997, **12**(2), 480–492.
30. Kondo, N., Ohji, T., Sato, E. and Wakai, F., Microstructures and mechanical properties of anisotropic silicon nitride produced by superplastic deformation. *Key Eng. Mater.*, 1999, **161–163**, 555–558.
31. Kondo, N., Ohji, T. and Wakai, F., Superplastic forging of silicon nitride ceramics with anisotropic microstructure control. *J. Mat. Sci. Lett.*, 1998, **17**, 45–47.
32. Kondo, N., Sato, E. and Wakai, F., Geometrical microstructural development in superplastic silicon nitride with rod-shaped grains. *J. Am. Ceram. Soc.*, 1998, **81**(12), 3221–3227.

33. Hay, J. C., Sun, E. Y., Pharr, G. M., Becher, P. F. and Alexander, K. B., Elastic anisotropy of beta-silicon nitride whiskers. *J. Am. Ceram. Soc.*, 1998, **81**(10), 2661–2669.
34. Ohji, T., Hirao, K. and Kanzaki, S., Fracture resistance behavior of highly anisotropic silicon nitride. *J. Am. Ceram. Soc.*, 1995, **78**(11), 3125–3128.
35. Becher, P. F., Microstructural design of toughened ceramics. *J. Am. Ceram. Soc.*, 1991, **74**(2), 255–269.
36. Becher, P. F., Hwang, S. L., Lin, H. T. and Tiegs, T. N., Microstructural contribution to the fracture resistance of silicon nitride ceramics. In *Tailoring of Mechanical Properties of Si_3N_4 Ceramics*, ed. M. J. Hoffmann and G. Petzow. Kluwer Academic, The Netherlands, 1994, pp. 87–100.
37. Steinbrech, R. W., Toughening mechanisms for ceramic materials. *J. Eur. Ceram. Soc.*, 1992, **10**(3), 131–142.
38. Ohji, T., Kondo, N., Suzuki, Y. and Hirao, K., Grain bridging of highly anisotropic silicon nitride. *Mat. Lett.*, 1999, **40**, 5–10.